Dynamics anomaly in high-density amorphous ice between 0.7 and 1.1 GPa

Philip H. Handle and Thomas Loerting*

Institute of Physical Chemistry, University of Innsbruck, Innrain 80-82, A-6020 Innsbruck, Austria

(Received 15 September 2015; revised manuscript received 4 December 2015; published 12 February 2016)

We studied high-density amorphous ices between 0.004 and 1.6 GPa by isobaric *in situ* volumetry and by subsequent *ex situ* x-ray diffraction and differential scanning calorimetry at 1 bar. Our observations indicate two processes, namely, relaxation in the amorphous matrix and crystallization, taking place at well-separated time scales. For this reason, we are able to report rate constants of crystallization k_X and glass-transition temperatures T_g in an unprecedented pressure range. T_g's agree within ± 3 K with earlier work in the small pressure range where there is overlap. Both T_g and k_X show a pressure anomaly between 0.7 and 1.1 GPa, namely, a k_X minimum and a T_g maximum. This anomalous pressure dependence suggests a continuous phase transition from high- (HDA) to very-high-density amorphous ice (VHDA) and faster hydrogen bond dynamics in VHDA. We speculate this phenomenology can be rationalized by invoking the crossing of a Widom line between 0.7 and 1.1 GPa emanating from a low-lying HDA-VHDA critical point. Furthermore, we interpret the volumetric relaxation of the amorphous matrix to be accompanied by viscosity change to explain the findings such that the liquid state can be accessed prior to the crystallization temperature T_X at <0.4 GPa and >0.8 GPa.

DOI: 10.1103/PhysRevB.93.064204

I. INTRODUCTION

Amorphous ices are ubiquitous in space and are of importance in understanding the processes accompanying agglomeration of interstellar dust, star formation, and evolution of molecules [1]. In order to understand water's anomalies two liquids are invoked in some theories. A sharp, but continuous [2] or a first-order transition between these two liquids [3] was first suggested to take place at high-pressure conditions in theory. That is, the pressure variable has to be considered carefully in order to obtain a comprehensive picture. At moderately high pressure of about 0.07 GPa the spontaneous formation of a sharp interface in noncrystalline water, i.e., a first-order transition, was observed at 140 K in experiments [4]. This might be the signature of the predicted liquid-liquid transition between low- (LDL) and high-density liquid water (HDL), or alternatively the polyamorphic transformation between low-density amorphous ice (LDA) [5] and high-density amorphous ice (HDA) [6]. At even higher pressure, very-high-density amorphous ice (VHDA) was discovered as the third amorphous form of ice [7]. VHDA could represent the dynamically arrested form of a third liquid form of the one-component system H_2O, very-high-density liquid water (VHDL). However, it is still a matter of debate whether the relation between HDA and VHDA is similar to the polyamorphic relation between LDA and HDA. Some argue for a continuous nature of the transition between HDA and VHDA [8–12] whereas others see a weakly discontinuous character of this transition [7,13–15]. The questions "Is VHDA a distinct form of amorphous water?" and "Is noncrystalline water a liquid at atmospheric pressure and in the temperature range from 140 to 150 K?" were chosen to be two of the five key unanswered questions in our understanding of water anomalies by Debenedetti [16]. Both of these questions are addressed in the current work, where the latter question is even extended to the experimentally challenging high-pressure and low-temperature domain. A definitive answer to the question has been hampered by two issues. First, the proximity of the crystallization line T_X prevents the possibility of studying noncrystalline water at higher temperature. Even the rate constant of crystallization k_X associated with crossing the T_X line has not been quantified yet, except for some work in the vacuum on thin films [17–20]. Second, there is a lack of knowledge about the glass-transition temperature, separating the amorphous solid from the ultraviscous liquid state, at high-pressure conditions. Some even argue for a nanocrystalline nature of amorphous ices, i.e., no relation between amorphous ices and liquids (reviewed in Ref. [21]). At ambient pressure the calorimetric glass-transition temperature of 136 K and a crystallization temperature of 150 K suggest a relatively narrow window, in which LDL can be accessed from LDA [22–24]. In case of HDA and its glass transition to HDL recently some progress was made both at ambient pressure [25] and at high pressures up to 0.3 GPa [26,27]. These experiments suggest two distinct glass-transition temperatures T_g, where HDA's T_g is lower by about 20 K compared to LDA's T_g at ambient pressure [25]. This distinct nature is also seen in the pressure dependence of T_g, where LDA's T_g decreases and HDA's T_g increases with pressure at <0.3 GPa [28]. At >0.3 GPa there is barely any information about water's glass transition, with the notable exception of dielectric relaxation [29] and heat capacity measurements [30] of VHDA at 1 GPa by Andersson and Inaba. In order to establish the nature of the relationship between HDA and VHDA the largely unknown pressure dependence of k_X and T_g needs to be established. Thus, we here study the crystallization and relaxation kinetics of amorphous ices in an unprecedented broad pressure interval, up to 1.6 GPa. We do this by using *in situ* volumetry on the amorphous ices upon slow isobaric

*Corresponding author: thomas.loerting@uibk.ac.at

Published by the American Physical Society under the terms of the Creative Commons Attribution 3.0 License. Further distribution of this work must maintain attribution to the author(s) and the published article's title, journal citation, and DOI.

heating. From the volumetric curves we extracted relaxation and crystallization rate constants simultaneously because we have found them to be separated by orders of magnitude. These *in situ* measurements are accompanied by *ex situ* differential scanning calorimetry (DSC) and powder x-ray diffraction (XRD) analysis of the sample, in order to analyze the structural state and the thermal stability of the states encountered along the volumetry curves.

II. EXPERIMENTAL DETAILS

For the sample preparation 500 µl of ultrapure water were frozen to hexagonal ice at 77 K in a preformed indium container made from about 300 mg of indium foil of thickness 0.1 mm. The sample container was then pushed into a steel cylinder of bore diameter 8 mm, precompacted by compressing at 77 K to 1.0 GPa and then compressed to 1.5–1.7 GPa where pressure-induced amorphization takes place [6] yielding unannealed HDA (uHDA). Starting from the uHDA formed in this procedure we have either converted the sample to very-high-density amorphous ice (VHDA) [7] or to expanded HDA (eHDA, 0.1 GPa) [31], following the well-established procedures from our past work [4,7]. This step is necessary to increase the crystallization resistance of the samples, allowing us to study relaxation up to higher temperatures, as shown in our earlier work [32]. VHDA samples were then studied by isobaric heating at $0.004 \leqslant p \leqslant 0.70$ GPa, whereas eHDA samples were isobarically heated at $1.1 \leqslant p \leqslant 1.6$ GPa, both at a rate of $3\,\mathrm{K\,min^{-1}}$. That is, we do not start with the "amorphous equilibrium matrix" but monitor the relaxation toward this metastable "equilibrated state." In other words, we on purpose prepare an amorphous ice that is metastable with respect to another form of amorphous ice, but remains stable because of the kinetical arrest at 77 K. Upon heating, the constraint of kinetical arrest is released, leading to the irreversible transformation to the more stable amorphous form. The onset of volumetric changes associated with the onset of relaxation dynamics is used to infer the glass-transition temperature T_g. Above a certain temperature, crystallization then interferes and suddenly ends the equilibration process within the noncrystalline domain, bringing the system to its true equilibrium, the high-pressure crystalline state. *In situ* dilatometry curves are plotted as change-of-volume curves and corrected for the apparatus behavior by subtracting a blind experiment (cf. Ref. [33]). All samples from both paths were characterized by *ex situ* DSC and XRD measurements after quench recovery from different points of the volume curves (see Supplemental Material [34]).

T_g and the rate of crystallization k_X are then extracted from the volumetric processes by fitting the observations. To this end we use the following equation that has been developed in our earlier work [35]:

$$\Delta V_\mathrm{m}(t) = \sum_i \Delta_\mathrm{e} V_{\mathrm{m},i}\left(1 - \mathrm{e}^{-\left(\frac{\Xi_i(t)}{Rq\tau_{R,\infty,i}}\right)^{\beta_{p,i}^{V_\mathrm{m}}}}\right) + \propto_p^{V_\mathrm{m}} [T(t) - T_0]. \quad (1)$$

The function

$$\Xi_i(t) = E_{A,i}\left\{\mathrm{Ei}\left[-\frac{E_{A,i}}{RT(t)}\right] - \mathrm{Ei}\left(-\frac{E_{A,i}}{RT_0}\right)\right\} + R\left[T(t)\mathrm{e}^{-\frac{E_{A,i}}{RT(t)}} - T_0\mathrm{e}^{-\frac{E_{A,i}}{RT_0}}\right], \quad (2)$$

was used in the exponent and $\mathrm{Ei}(x)$ is the exponential integral:

$$\mathrm{Ei}(x) = \int_{-\infty}^{x} \frac{e^\xi}{\xi} d\xi. \quad (3)$$

The sum in the fitting function (1) has either only one ($i = 1$, i.e., relaxation only) or two exponential terms ($i = 2$, i.e., relaxation and crystallization), depending on whether or not the sample was heated high enough to observe the crystallization step in the experiments. The fitting function for $i = 1$ is the same we used and explained in detail recently [35] and it is deduced from a temperature-dependent first-order kinetic equation with the addition of a linear term (scaled with $\alpha_p^{V_\mathrm{m}}$) and an empirical exponent $\beta_p^{V_\mathrm{m}}$ similar to the well-established Kohlrausch-Williams-Watts (KWW) function (cf., e.g., Refs. [36–39]). The remaining quantities are the total time-dependent molar volume change $\Delta V_\mathrm{m}(t)$, the magnitude of the individual contributions $\Delta_\mathrm{e} V_{\mathrm{m},i}$, the individual activation energies $E_{A,i}$ and preexponential constants $\tau_{R,\infty,i}$, the starting temperature T_0, the ideal gas constant R, and the heating rate q. The volume curves were fitted as functions of temperature with the CURVE FITTING TOOLBOX of MATLAB R2013A, where $\Delta_\mathrm{e} V_{\mathrm{m},i}$, $E_{A,i}$, $\tau_{R,\infty,i}$, $\propto_p^{V_\mathrm{m}}$, and $\beta_p^{V_\mathrm{m}}$ were used as fitting parameters.

Here the exponent $\beta_p^{V_\mathrm{m}}$ plays a central role, because we interpret processes with $\beta_p^{V_\mathrm{m}} \geqslant 1$ (faster than a regular first-order kinetic) to indicate a first-order phase-transition, whereas $\beta_p^{V_\mathrm{m}} < 1$ (slower than a regular first-order kinetic) as indication of a relaxation. Examples of fit curves are shown in Figs. 1 and 2 and all fitting parameters are summarized in Tables SM1 and SM2 (see Supplemental Material [34]). From these fits we obtained separate activation energies E_A and time scales $\tau_{R,\infty}$ of the relaxation processes ($\beta_p^{V_\mathrm{m}} < 1$) and crystallizations ($\beta_p^{V_\mathrm{m}} \geqslant 1$; $p \geqslant 0.1$ GPa) at different pressures. From the parameters E_A and $\tau_{R,\infty}$ corresponding to the relaxation we estimate the glass-transition temperatures at the respective pressures via

$$\tau_R(T_g) = \tau_{R,\infty} e^{\frac{E_A}{RT_g}} = 100\,\mathrm{s}. \quad (4)$$

Using a τ_R of 100 s for the definition of T_g put to work here is a convention used by several authors (cf., e.g., Refs. [25,29,36,38–40]. The use of the Arrhenius equation is further justified for HDA since Amann-Winkel *et al.* classified HDL as a strong liquid (steepness index $m = 20$–25) near the glass transition [25] and because relaxation of a solid glass is typically an activated process [36].

We are furthermore able to extract rate constants for crystallization k_X as a function of pressure and temperature from the parameters E_A and $\tau_{R,\infty}$ corresponding to the crystallization using

$$k_X(T) = \frac{1}{\tau_{R,\infty}} e^{-\frac{E_A}{RT}}. \quad (5)$$

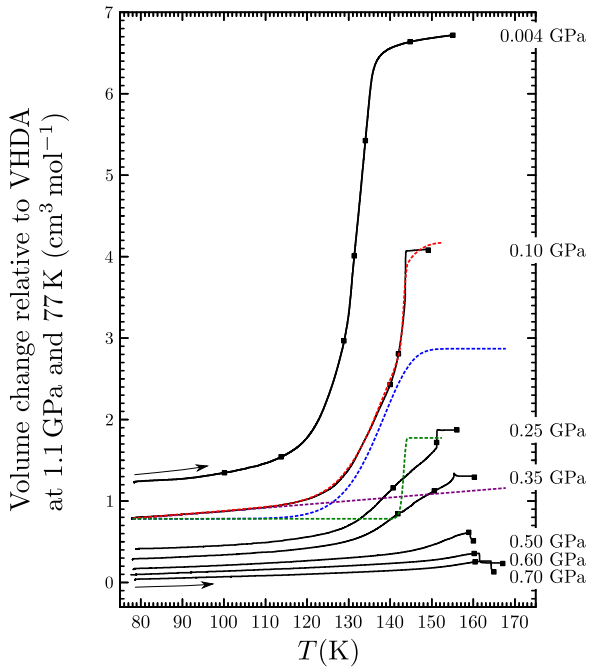

FIG. 1. Change of the molar volume relative to VHDA at 1.1 GPa and 77 K during isobaric heating. The points mark additional experiments for *ex situ* XRD and DSC characterization. For the volume curve at 0.1 GPa also the fit with Eq. (1) is shown ($i = 2$, red dashed curve). For this fit also all contributing terms are drawn separately: First exponential term ($\beta_p^{V_m} \approx 0.6$, blue dashed curve; relaxation), second exponential term ($\beta_p^{V_m} \approx 8$, green dashed curve; crystallization), linear term (purple dashed curve; thermal expansion).

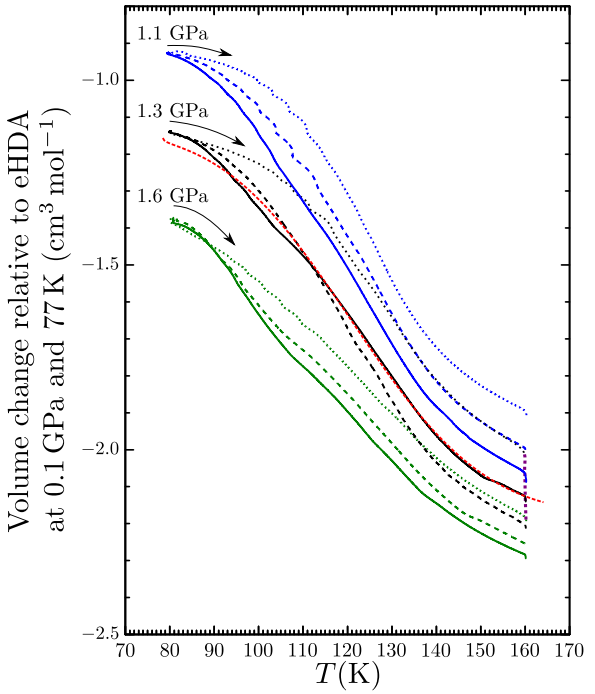

FIG. 2. Change of the molar volume relative to eHDA at 0.1 GPa and 77 K during isobaric heating. The dotted lines represent experiments of variant (n), the dashed lines of variant (s), and the solid lines of variant (st) (see Supplemental Material [34]). *Ex situ* XRD and DSC characterizations have been conducted on all nine samples after subsequent quench recovery (see Supplemental Material [34]). For the volume curve at 1.3 GPa [(st), solid black line] also the fit with Eq. (1) is shown ($i = 1$, red dashed line).

III. RESULTS AND DISCUSSION

A. Qualitative description of the VHDA → eHDA and the eHDA → VHDA conversions

The volumetric behavior of VHDA during heating is shown in Fig. 1. Clearly the samples expand at all pressures, most strongly at the low-pressure end. All curves exhibit a continuous expansion followed by a sharp step. The DSC and XRD characterizations (see Supplemental Material [34]) from quench-recovered samples demonstrate the steps are due to crystallization, except at 0.004 GPa, where the step is due to the polyamorphic transformation to LDA. The continuous expansion is identified as relaxation that manifests itself in a continuous shift of the halo peak in XRD experiments and a shift in transformation temperature in DSC experiments. The *ex situ* characterization indicates that VHDA continuously relaxes and reaches an expanded HDA state, called eHDA [31], at 0.2–0.7 GPa. This state represents a HDA state at or close to metastable equilibrium [4].

The volumetric behavior of eHDA during heating at $\geqslant$1.1 GPa is shown in Fig. 2. Each measurement was conducted in three slightly different ways, e.g., using different rates of compression and different thicknesses of the indium container (see Supplemental Material [34]). The measurements show the same qualitative behavior, with only small variations. Here a continuous densification rather than expansion is observed in this pressure interval. At the high-temperature end near 160 K the densification slows down. This suggests a metastable equilibrium state to be reached prior to crystallization. The XRD and DSC characteristics of this state are those of VHDA, suggesting eHDA relaxes towards VHDA, the equilibrated amorphous ice state at $\geqslant$1.1 GPa. Crystallization of the equilibrated state manifests itself as a sharp step in all cases (see Fig. 1 and portion of the curve highlighted in violet on the black dotted line in Fig. 2). The DSC and XRD characterizations after subsequent quench recovery indicate clearly the amorphous nature prior to the step, although some crystalline traces appear (see Supplemental Material [34]). By contrast, the samples exhibit a fully crystalline nature after heating beyond the step.

In other words, the VHDA samples at <0.7 GPa relax and expand towards eHDA before they crystallize, whereas the eHDA samples at $\geqslant$1.1 GPa relax and densify towards VHDA before they crystallize. Furthermore, there is no discontinuity in the eHDA ↔ VHDA conversion upon isobaric heating apparent in Figs. 1 and 2. The only discontinuity observed in our experiments is related to crystallization ($p \geqslant 0.1$ GPa) or to transformation to LDA ($p = 0.004$ GPa).

B. Discussion of extracted T_g

The broad and slow relaxation process contrasts the sharp and fast crystallization process. The large separation between time scales indicated by this observation allows us to single out the individual contributions from relaxation and crystallization

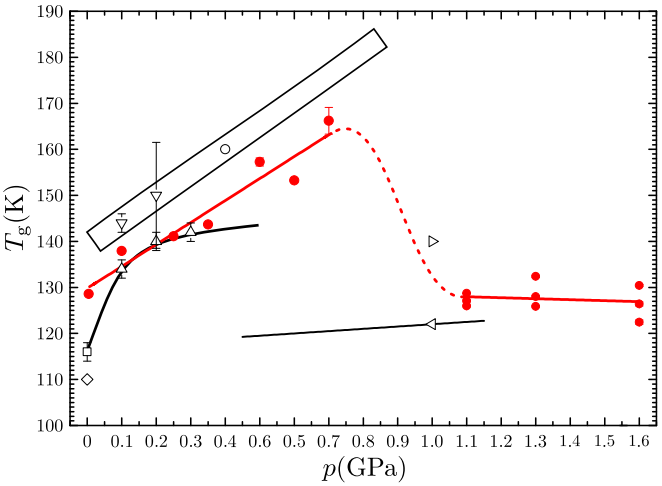

FIG. 3. Estimated glass-transition temperatures (red circles). The red solid and dotted lines are a guide to the eye. Additionally literature data are shown for comparison: T_g for eHDA determined by DSC ($q = 10\,\mathrm{K\,min^{-1}}$; open square) [25]; by dielectric relaxation ($q \approx 0.01\,\mathrm{K\,min^{-1}}$; open diamond) [25]; by high-pressure volumetry ($q = 2\,\mathrm{K\,min^{-1}}$; open upward triangles) [26]; for uHDA determined by relaxation on basis of *ex situ* DSC measurements (open downward triangles) [27]; and glass-transition temperatures for VHDA determined by temperature change during decompression (rate $= 0.2\,\mathrm{GPa\,min^{-1}}$; open circle) at 160 K and extrapolation (black rectangle) [47]; high-pressure dielectric relaxation ($q = 15\,\mathrm{K\,h^{-1}}$; open left triangle) with extrapolation (black line) [29]; by the transient hot-wire method ($q = 0.4\,\mathrm{K\,min^{-1}}$; open right triangle) [30]. The black line at lower pressures ($p < 0.6\,\mathrm{GPa}$) shows the expected $T_g(p)$ progression for HDA according to the ST2 water model [28].

to the volumetric changes by using the fit function (1) detailed in the Experimental Details section as a function of time t or temperature $T(t)$. Furthermore the glass-transition temperatures T_g can be extracted using the definition of a relaxation time of 100 s. The T_g's obtained in this way are shown in Fig. 3 alongside experimental literature data. In the pressure range up to 0.3 GPa there is a very good agreement of the data extracted using our procedure here with literature data. The definition of T_g used in this work is based on irreversible volume changes, while it was based on reversible changes of the thermal expansion coefficient in our earlier work [26] or on a heat capacity step at 1 GPa in the work by Andersson [30]. In spite of this very different criterion indicating the molecular mobility at T_g there is an excellent agreement between the methods. This shows that the criterion used in this work is valid, in spite of it being based on irreversible relaxation processes. In absolute numbers the T_g data reported here are accurate within ± 3 K. Similarly, upon changing the experimental procedure we find the variation of resulting T_g values to be within ± 3 K, indicating the minor influence of the changed parameters and the robustness of our fit procedure for the volumetric changes (see Supplemental Material [34]). We regard these error bars as minor, given the scarcity of data in this pressure interval and the challenging task of obtaining T_g in high-p, low-T experiments. At >0.3 GPa there is almost no information about T_g in literature, where we report an unprecedented large body of data here in Fig. 3. The increase of T_g with pressure reported in earlier work up to 0.3 GPa [26,27] continues at least up to 0.7 GPa. In this pressure interval we see a crossing of the T_g and T_X lines at 0.4 GPa; i.e., the liquid state above T_g cannot be reached in bulk water prior to crystallization above 0.4 GPa. This is in agreement with the earlier conclusion by Seidl *et al.* [26,27]. The T_gs obtained at $\geqslant 1.1$ GPa are almost constant at 127 ± 3 K, i.e., about 30 K lower than the value at 0.7 GPa, a drop ten times as large as the estimated uncertainty for our T_gs. No discontinuities are found for both the VHDA $\rightarrow$ eHDA and the eHDA $\rightarrow$ VHDA conversion here. However, there is a sharp drop of T_g above 0.7 GPa, which we regard to be continuous. This drop represents a pressure anomaly in water's relaxation dynamics and is not expected according to most theories explaining the glass transition, e.g., free volume theories. That is, at ≈ 0.8 GPa there is another crossing between T_g and T_X such that the ultraviscous liquid can again be accessed prior to crystallization at >0.8 GPa. This also resolves the apparent contradiction why Seidl *et al.* stated that it is not possible to access the liquid state at $\geqslant 0.4$ GPa [26,27], whereas Andersson reported evidence for the liquid state under high pressure of 1 GPa [30].

In order to rationalize this surprising finding of the turnaround of the T_g line we invoke a phase transition, specifically the transition from HDA to VHDA, which is reported to take place in a narrow pressure range around 0.8 GPa upon increasing pressure [7,14,33]. The sharp drop in T_g implies that hydrogen bond dynamics is much faster in VHDA than in HDA. That is, VHDA and HDA have to be considered two distinct amorphous ices differing in terms of water mobility [15]. This conclusion is consistent with the earlier conclusion of a longer O-O distance and weaker hydrogen bonds in VHDA than in HDA at 1 bar [7]. However, VHDA and HDA are not connected by a first-order-like transition, as is the case for LDA-HDA. These two amorphous ices are, instead, continuously connected according to our isobaric experiments, and depending on pressure either VHDA is formed from HDA by a continuous process or vice versa, consistent with theoretical [41,42] and experimental [8–12] work. Still, VHDA and HDA are clearly distinct; in particular there is a jumplike change of the isothermal compressibility near 0.8 GPa, and here we reveal the sudden change in hydrogen bond dynamics between 0.7 and 1.1. GPa [13]. The continuous process together with the $T_g(p)$ maximum leads us to the speculation of a low-lying critical point near 0.8 GPa, where a binodal representing equal Gibbs free energies for HDA and VHDA might end. The continuous nature would then imply a crossing of the Widom line emanating from the low-lying critical point. This point is expected to be located at temperatures below 77 K. We emphasize this is a speculation which is consistent with our experimental results collected here and in our earlier work. It is clearly not a rigorous proof, and this explanation is not the only way of rationalizing a maximum in $T_g(p)$. There have been studies in which such an observation was explained without explicitly referring to a low-lying critical point [43,44]. However, in conjunction with the evidence from earlier work about the distinct nature of HDA and VHDA, including the mapping of the transition between the two, we suggest this to be the best explanation for the findings [10] by now.

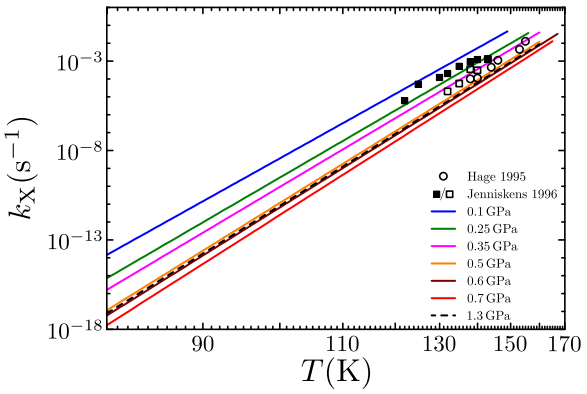

FIG. 4. Crystallization rate constants k_X in comparison with literature data for HGW [18] and ASW [19]. Please note that our rate constants combine nucleation and growth. We do not know whether growth or nucleation is the rate-limiting step, and so we refrain from reporting nucleation rates.

C. Discussion of extracted k_X

The estimates for $k_X(T)$ are shown in Fig. 4 and compared with measurements on hyperquenched glassy water (HGW) and amorphous solid water (ASW), both of which represent low-density amorphous ice forms. Please note, we here report rates of crystallization, but cannot say whether these rates are nucleation limited or growth limited. Hence, we do not report nucleation rates of amorphous ices as was done in earlier work [45]. The rate constants obtained here for HDA are comparable to those of ASW and HGW measured earlier [18,19] and are expected to be accurate within a few percent, except for 1.3 GPa where a larger deviation is possible. When increasing the pressure from 0.1 GPa to 0.7 GPa, k_X drops by about four orders of magnitude, but then increases again by about an order of magnitude upon increasing the pressure further to 1.3 GPa (see Fig. 4). These changes are much larger than the uncertainties of the procedure, and so clearly k_X has a minimum at or slightly above 0.7 GPa. This represents the second manifestation of the pressure anomaly in water's dynamics reported in the present work. Again the apparent continuum of states between HDA and VHDA requires continuous $k_X(p)$ progression. We rationalize the minimum by noting that the slowest crystallization is observed at 0.7 GPa, where also the highest T_g was found (see Fig. 3). If T_g indicates a glass-liquid transition, viscosity is highest and accordingly mobility of water molecules lowest, and as a result crystallization kinetics is slowest at 0.7 GPa. Both at <0.7 GPa and at 1.3 GPa T_g is lower than at 0.7 GPa (see Fig. 3), so that viscosity is lower and accordingly water mobility higher and crystallization kinetics faster in VHDA than in HDA. In other words, the anticorrelation of T_g and k_X trends with pressure in Figs. 3 and 4 suggests the glass transition of HDA and VHDA is indeed caused by a process affecting viscosity and involving ultraviscous liquid nature above T_g. This contrasts claims in the literature that the glass transition is not related to viscosity changes, but to orientational order of water molecules in the glass (see Ref. [21] for a review).

IV. CONCLUSION

We studied isobaric conversions from VHDA to eHDA at $0.004 \leqslant p \leqslant 0.70$ GPa and from eHDA to VHDA at $1.1 \leqslant p \leqslant 1.6$ GPa. These conversions take place as relaxations without discontinuities indicating a continuum of states in the studied p-T area. Furthermore, we studied the second process competing with relaxation, namely, crystallization of eHDA and VHDA. The two processes are well separated in terms of time scales so that parameters describing both processes independently can be extracted from volumetric curves recorded on isobaric heating. This allows us to report the pressure dependence of the glass-transition temperature T_g at pressures up to 1.6 GPa and to identify an anomaly between 0.7 and 1.1 GPa. Namely, T_g increases rather linearly up to 0.7 GPa, where it reaches about 160 K. In the pressure interval between 0.7 and 1.1 GPa T_g then turns around and drops by about 30 K. This behavior is peculiar and very hard to reconcile without assuming an underlying additional transition, which is identified to be the HDA → VHDA transition [15]. For comparison the error bar associated with the method is ±3 K, based both on a comparison with literature data and on varying experimental parameters slightly. These findings resolve apparent inconsistencies in the literature, in particular the increase of HDA's T_g with pressure, which seemed to be at odds with the low-lying T_g reported by Andersson and Inaba at 1 GPa [29]. In other words, due to the largely different hydrogen-bond dynamics in HDA and VHDA revealed here, we have to consider the glass-transition temperatures for HDA and VHDA as distinct, where VHDA's T_g is much lower than HDA's T_g. This makes the case for HDA and VHDA to be distinct polyamorphic forms—in accordance with the conclusion made by Finney in his recent book [46]. Furthermore, we report a set of crystallization rate constants k_X for eHDA and VHDA at 0.1–1.3 GPa. Consistently with the T_g data from Fig. 3 the k_X data from Fig. 4 reveal a pressure anomaly between 0.7 and 1.3 GPa, namely, a minimum. We interpret this to indicate that viscosity changes affect crystallization rates such that there is a faster crystallization in less viscous material; i.e., that HDA above T_g is in its ultraviscous liquid HDL state at crystallization. The liquid state below the crystallization temperature T_X can only be equilibrated and accessed in the pressure intervals $p < 0.4$ GPa and $p > 0.8$ GPa. In between, the glass-transition temperature T_g is found to be above T_X; i.e., $T_g > T_X$ at $0.4 < p < 0.8$ GPa. At <0.4 GPa a liquid resembling eHDA can be accessed, at >0.8 GPa a liquid resembling VHDA. The questions raised by Debenedetti [16] can, thus, be answered as follows. "Is VHDA a distinct form of amorphous water?": Yes, it clearly is as evidenced by the sudden change in thermal expansivity and hydrogen-bond dynamics near 0.8 GPa. However, at >77 K the transition is continuous, not first-order-like. "Is noncrystalline water a liquid at atmospheric pressure and in the temperature range from 140 to 150 K?": Our recent work [1,24,26] suggests this to be the case for the low-density liquid state near ambient pressure, and the present work suggests that also at high pressures a high-density liquid state can be accessed prior to crystallization, except between 0.4 and 0.8 GPa.

ACKNOWLEDGMENTS

We are thankful for financial support by the Austrian Science Fund FWF (project I1392 and START award Y391).

[1] C. Mitterdorfer, M. Bauer, T. G. A. Youngs, D. T. Bowron, C. R. Hill, H. J. Fraser, J. L. Finney, and T. Loerting, Phys. Chem. Chem. Phys. **16**, 16013 (2014).

[2] S. Sastry, P. G. Debenedetti, F. Sciortino, and H. E. Stanley, Phys. Rev. E **53**, 6144 (1996).

[3] P. H. Poole, F. Sciortino, U. Essmann, and H. E. Stanley, Nature **360**, 324 (1992).

[4] K. Winkel, E. Mayer, and T. Loerting, J. Phys. Chem. B **115**, 14141 (2011).

[5] O. Mishima, L. D. Calvert, and E. Whalley, Nature **314**, 76 (1985).

[6] O. Mishima, L. D. Calvert, and E. Whalley, Nature **310**, 393 (1984).

[7] T. Loerting, C. Salzmann, I. Kohl, E. Mayer, and A. Hallbrucker, Phys. Chem. Chem. Phys. **3**, 5355 (2001).

[8] O. Mishima, Nature **384**, 546 (1996).

[9] S. Klotz, G. Hamel, J. S. Loveday, R. J. Nelmes, M. Guthrie, and A. K. Soper, Phys. Rev. Lett. **89**, 285502 (2002).

[10] T. Loerting, K. Winkel, C. G. Salzmann, and E. Mayer, Phys. Chem. Chem. Phys. **8**, 2810 (2006).

[11] K. Winkel, M. S. Elsaesser, E. Mayer, and T. Loerting, J. Chem. Phys. **128**, 044510 (2008).

[12] Y. Suzuki and Y. Tominaga, J. Chem. Phys. **133**, 164508 (2010).

[13] C. G. Salzmann, T. Loerting, S. Klotz, P. W. Mirwald, A. Hallbrucker, and E. Mayer, Phys. Chem. Chem. Phys. **8**, 386 (2006).

[14] T. Loerting, W. Schustereder, K. Winkel, C. G. Salzmann, I. Kohl, and E. Mayer, Phys. Rev. Lett. **96**, 025702 (2006).

[15] T. Loerting, K. Winkel, M. Seidl, M. Bauer, C. Mitterdorfer, P. H. Handle, C. G. Salzmann, E. Mayer, J. L. Finney, and D. T. Bowron, Phys. Chem. Chem. Phys. **13**, 8783 (2011).

[16] P. G. Debenedetti, J. Phys.: Condens. Matter **15**, R1669 (2003).

[17] W. Hage, A. Hallbrucker, E. Mayer, and G. P. Johari, J. Chem. Phys. **100**, 2743 (1994).

[18] W. Hage, A. Hallbrucker, E. Mayer, and G. P. Johari, J. Chem. Phys. **103**, 545 (1995).

[19] P. Jenniskens and D. F. Blake, Astrophys. J. **473**, 1104 (1996).

[20] D. J. Safarik and C. B. Mullins, J. Chem. Phys. **121**, 6003 (2004).

[21] T. Loerting, V. Fuentes-Landete, P. H. Handle, M. Seidl, K. Amann-Winkel, C. Gainaru, and R. Böhmer, J. Non-Cryst. Solids **407**, 423 (2015).

[22] J. A. McMillan and S. C. Los, Nature **206**, 806 (1965).

[23] G. P. Johari, A. Hallbrucker, and E. Mayer, Nature **330**, 552 (1987).

[24] M. S. Elsaesser, K. Winkel, E. Mayer, and T. Loerting, Phys. Chem. Chem. Phys. **12**, 708 (2010).

[25] K. Amann-Winkel, C. Gainaru, P. H. Handle, M. Seidl, H. Nelson, R. Bohmer, and T. Loerting, Proc. Natl. Acad. Sci. USA **110**, 17720 (2013).

[26] M. Seidl, M. S. Elsaesser, K. Winkel, G. Zifferer, E. Mayer, and T. Loerting, Phys. Rev. B **83**, 100201 (2011).

[27] P. H. Handle, M. Seidl, and T. Loerting, Phys. Rev. Lett. **108**, 225901 (2012).

[28] N. Giovambattista, T. Loerting, B. R. Lukanov, and F. W. Starr, Sci. Rep. **2**, 390 (2012).

[29] O. Andersson and A. Inaba, Phys. Rev. B **74**, 184201 (2006).

[30] O. Andersson, Proc. Natl. Acad. Sci. USA **108**, 11013 (2011).

[31] R. J. Nelmes, J. S. Loveday, T. Straessle, C. L. Bull, M. Guthrie, G. Hamel, and S. Klotz, Nat. Phys. **2**, 414 (2006).

[32] M. Seidl, A. Fayter, J. N. Stern, G. Zifferer, and T. Loerting, Phys. Rev. B **91**, 144201 (2015).

[33] K. Winkel, W. Schustereder, I. Kohl, C. G. Salzmann, E. Mayer, and T. Loerting, in *Proceedings of the 11th International Conference on the Physics and Chemistry of Ice*, edited by W. F. Kuhs (RSC, Dorchester, UK, 2007), p. 641.

[34] See Supplemental Material at http://link.aps.org/supplemental/10.1103/PhysRevB.93.064204 for four figures detailing *ex situ* DSC and XRD characterization of all samples, which include additional experiments to analyze the influence of slower compression (s) and thicker indium container walls (st). In addition, two tables detail the fitting procedure and the robustness of the results against variation of compression rate and container wall thickness.

[35] P. H. Handle and T. Loerting, Phys. Chem. Chem. Phys. **17**, 5403 (2015).

[36] I. M. Hodge, J. Non-Cryst. Solids **169**, 211 (1994).

[37] C. T. Moynihan, Rev. Mineral. Geochem. **32**, 1 (1995).

[38] C. A. Angell, K. L. Ngai, G. B. McKenna, P. F. McMillan, and S. W. Martin, J. Appl. Phys. **88**, 3113 (2000).

[39] P. G. Debenedetti and F. H. Stillinger, Nature **410**, 259 (2001).

[40] M. I. Ojovan, Adv. Condens. Matter Phys. **2008**, 817829 (2008).

[41] R. Martonak, D. Donadio, and M. Parrinello, Phys. Rev. Lett. **92**, 225702 (2004).

[42] R. Martonak, D. Donadio, and M. Parrinello, J. Chem. Phys. **122**, 134501 (2005).

[43] A. Drozd-Rzoska, S. J. Rzoska, and A. R. Imre, J. Non-Cryst. Solids **353**, 3915 (2007).

[44] A. Drozd-Rzoska, S. J. Rzoska, M. Paluch, A. R. Imre, and C. M. Roland, J. Chem. Phys. **126**, 164504 (2007).

[45] H. Laksmono *et al.*, J. Phys. Chem. Lett. **6**, 2826 (2015).

[46] J. Finney, *Water: A Very Short Introduction* (Oxford University Press, Oxford, New York, 2015).

[47] O. Mishima, J. Chem. Phys. **121**, 3161 (2004).